THE JOURNAL OF PHYSICAL CHEMISTRY C

ARTICLE

pubs.acs.org/JPCC

Raman Spectroscopy of the Reaction of Thin Films of Solid-State Benzene with Vapor-Deposited Ag, Mg, and Al

Matthew C. Schalnat, Adam M. Hawkridge,† and Jeanne E. Pemberton*

Department of Chemistry and Biochemistry, University of Arizona, 1306 East University Boulevard, Tucson, Arizona 85721, United States

Supporting Information

ABSTRACT: Thin films of solid-state benzene at 30 K were reacted with small quantities of vapor-deposited Ag, Mg, and Al under ultrahigh vacuum, and products were monitored using surface Raman spectroscopy. Although Ag and Mg produce small amounts of metal−benzene adduct products, the resulting Raman spectra are dominated by surface enhancement of the normal benzene modes from metallic nanoparticles suggesting rapid Ag or Mg metallization of the film. In contrast, large quantities of Al adduct products are observed. Vibrational modes of the products in all three systems suggest adducts that are formed through a pathway initiated by an electron transfer reaction. The difference in reactivity between these metals is ascribed to differences in ionization potential of the metal atoms; ionization potential values for Ag and Mg are similar but larger than that for Al. These studies demonstrate the importance of atomic parameters, such as ionization potential, in solid-state metal−organic reaction chemistry.

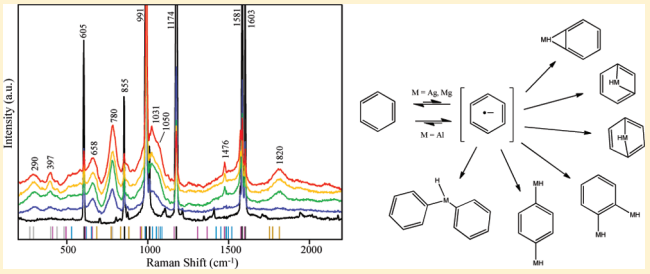

INTRODUCTION

The chemistry between reactive metal atoms such as Ag, Mg, and Al and organic molecules is relevant in multiple scientific contexts, including organometallic chemistry in the condensed[1−6] and gas phases,[7−10] biological systems,[11] interstellar media,[12−14] and geochemistry.[15,16] Indeed, numerous studies on the reactions of such metals with small organic molecules have been reported in the literature. These are typically performed on matrix-isolated metal atom−organic pairs[17−19] or on gas-phase metal cation−organic pairs.[20−22] Extensive theoretical work has also been published on such reactions.[23−29] Although this previous body of work documents the ability to study reaction chemistry of these reactive metals with organics, all previous studies have been restricted to one or two metal atoms or cations reacting with a single organic molecule. No attention to the course of such reactions for organic molecules in the solid-state has been reported, despite their potential relevance in astrochemical and geochemical situations and device technologies. Reactions of these metals with organics in the solid state may follow different pathways due to the proximity of a metal atom or cation to multiple organic molecules.

In this laboratory, interest in such chemistry is motivated by an interest in understanding and improving charge injection efficiency at metal−organic heterojunctions in devices such as organic light emitting diodes, organic photovoltaics, and organic field effect transistors. These devices often utilize metal contacts made from such reactive metals due to their relatively low work function. Toward this end, fundamental studies of interfaces formed between organic semiconductors or simple organic models, of these materials, and such low work function metals are being investigated using Raman spectroscopy. In previous efforts, we have reported on reactions between thin films of *trans*-stilbene and Al[30] and between tris(8-hydroxyquyinoline)aluminum (Alq_3) and Ag,[31] Al,[31] Mg,[32] and Ca.[33] These studies demonstrated the power of Raman spectroscopy for understanding this fundamental interfacial chemistry but also exposed the unanticipated complexity of such reactions. The challenges inherent in interpreting the reaction product spectra from molecules as simple as Alq_3 compelled further systematic investigation of the reactions of such metals with solid-state films of simpler organic molecules that are constituent parts of organic semiconductors. Thus, in the present study, the reactions of benzene with Ag, Mg, and Al are reported.

Previous studies on the reactions of benzene with reactive metals have been performed in the condensed phase,[34−40] in the gas phase,[22,41−46] and using matrix isolation.[18,47,48] Theoretical studies on these reactions have also been reported.[20,23,25,27,49−63] Collectively, this previous work documents reaction through an electron transfer pathway for isolated benzene molecules, and these studies have provided detailed information about the bonding in the metal−benzene complexes so formed. However, no previous work has addressed the details of this reaction chemistry for bulk solid-state benzene wherein proximity of multiple benzene molecules has the potential to alter the reaction pathway or the products formed.

Received: January 29, 2011
Revised: June 8, 2011
Published: June 09, 2011

Thus, the goal of the work reported here is to characterize the reactions of solid-state benzene thin films during the initial stages of metallization by Ag, Mg, and Al at 30 K using surface Raman spectroscopy. Insight from such studies is expected to contribute to a broader understanding of reaction chemistry that might occur at low work function metal−organic semiconductor interfaces important in the device technologies noted above. Surface Raman spectroscopy is used for these analyses because of its high molecular specificity and sensitivity to changes in structure and bonding accompanied by a wide spectral window allowing access to the low-frequency region that inherently contains information about metal−organic bonds.

EXPERIMENTAL SECTION

Materials. Benzene (99.9+%, HPLC grade) was purchased from Sigma Aldrich. Metals were purchased from Alfa Aesar in the form of Al foil (99.999% pure), Ag foil (99.999% pure), and Mg turnings (99.98% pure). Mg was shipped under Ar and introduced into ultrahigh vacuum (UHV) immediately upon receipt. H_2SO_4 (EM Science, ACS grade), Cr_2O_3 (98+%, Aldrich, ACS grade), HCl (37%, Mallinckrodt, ACS grade), NH_4OH (30% NH_3, Spectrum), and HNO_3 (Mallinckrodt, ACS grade) were used as received. Water was purified (resistivity >18 MΩ and organic contaminants <6 ppb) using a Waters Milli-Q UV Plus System (Millipore Corp.). Polycrystalline Ag surfaces were fabricated from 12.5 mm diameter Ag rods (Alfa Aesar, 99.9985%).

Ultrahigh Vacuum Chamber. Thin films were prepared and characterized in a custom-built UHV chamber described previously.[30−32] The vacuum system consists of three chambers: a sample entry chamber, a sample preparation chamber, and an analysis chamber. The preparation chamber was maintained at a base pressure of $<3 \times 10^{-10}$ Torr, and working pressures were seldom above 10^{-9} Torr. Base pressures in the analysis chamber were routinely maintained at 5×10^{-11} Torr.

Substrate Preparation. Smooth, chemically polished Ag substrates were used as substrates in these studies. These were prepared using a chemical cleaning method described previously from this laboratory.[64,65] Once prepared, these substrates were mounted on a custom-built translatable arm (DE-204B, Advanced Research Systems) and cooled to <30 K with a closed-cycle He cryogenic refrigerator (APD Cryogenics, model HC4). Substrate temperature was controlled using a cryogenic temperature controller (Cryo-Con model 34) coupled to a type K (Chromel-AuFe) thermocouple located in close proximity to the substrate surface.

Benzene thin films were dosed through a calibrated glass capillary array doser after three freeze−pump−thaw cycles. Benzene thicknesses, reported in uncorrected langmuirs,[66] were deposited at a rate of 0.2 langmuirs/s. Typical films were ∼5 monolayers (ML) in thickness (assuming 1 langmuir ≅ 1 ML), corresponding to $\sim 4.9 \times 10^{14}$ molecules/cm^2 of benzene. After acquisition of a Raman spectrum of the pristine benzene film, the surface was then exposed to sequential depositions of 5 Å mass thickness of the respective metal ($\sim 2.0 \times 10^{15}$ atoms/cm^2 of Ag and Al, and 1.4×10^{15} atoms/cm^2 of Mg assuming bulk density) up to 20 Å, with Raman spectra acquired after each deposition. Metal mass thicknesses were monitored with a liquid-N_2-cooled quartz crystal microbalance (Maxtek, Inc., model TM-400).

Raman Spectroscopy. Raman scattering was excited and collected using a previously described instrument.[32] Acquisition times were 10 min with a 5 cm^{-1} spectral bandpass. Peak fitting to a minimum number of bands per envelope was accomplished using a 40/60% Lorentzian/Gaussian peak shape and were deemed acceptable for $\chi^2 > 0.99$.

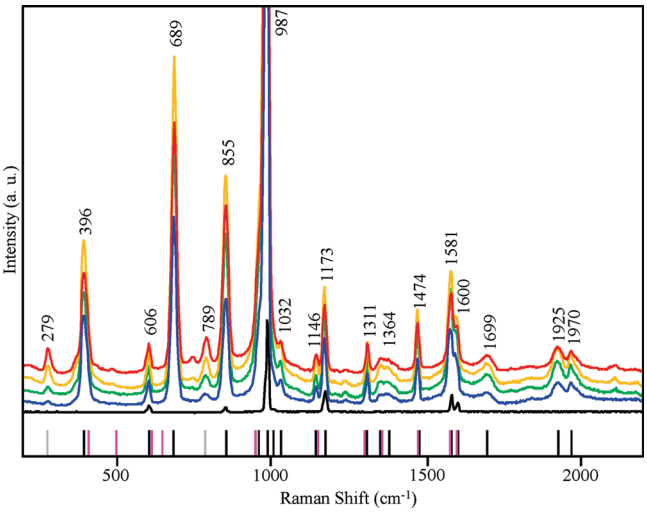

Figure 1. Raman spectra of a pristine 5 ML benzene thin film before (black) and after deposition of 5 (blue), 10 (green), 15 (orange), and 20 (red) Å mass thickness of Ag. Underlying tick marks identify characteristic frequencies for benzene (black), the benzene anion radical (pink), and the Ag−benzene adduct (gray).

RESULTS AND DISCUSSION

Raman spectra of thin, amorphous,[67] solid-state benzene films on Ag have been reported previously in the literature.[68,69] The full Raman spectrum between 150 and 2000 cm^{-1} from a 5 ML solid-state benzene film at 30 K is shown in Figure S1 of the Supporting Information. Seven bands assigned to six vibrational modes are sufficiently intense to be distinguished above the background, including the four in-plane modes of Wilson notation ν_1, ν_6, ν_8, ν_9, and ν_{12}, and one out-of-plane mode, ν_{10}. The most intense band is the $\nu(C-H)_{ring}$ mode (ν_1) centered at 991 cm^{-1}. The peak frequencies observed in this Raman spectrum are consistent with amorphous, solid-state benzene.[67−71]

Reaction of Ag and Mg with Benzene. Figures 1 and 2 show a series of Raman spectra between 150 and 2200 cm^{-1} from a 5 ML benzene film exposed to increasing mass thicknesses of vapor-deposited Ag and Mg, respectively. Table 1 contains the peak frequencies of bands observed in these spectra and their assignments. Two distinct effects of Ag and Mg postdeposition on the solid-state benzene film are noted in the spectra. The primary effect is surface enhancement of the Raman scattering of unreacted solid-state benzene modes (black tick marks below the spectra in Figure 1), presumably by metal nanoparticles formed during the initial stages of metallization. In addition to an intensity increase of the six Raman-active modes observed in the pristine film (ν_1, ν_6, ν_8, ν_9, ν_{10}, ν_{12}) due to surface enhancement, other in-plane (ν_3, ν_{14}, ν_{15}, ν_{18}, and ν_{19}) and out-of-plane (ν_5, ν_{11}, ν_{16}, and ν_{17}) modes are also observed after metal deposition. The activation of these normally Raman-inactive modes and the presence of ν_{11}, ν_{10}, ν_{17}, and ν_5 and their overtones near 1370, 1700, 1925, and 1970 cm^{-1} are indications of surface enhanced Raman scattering along with a reduction in benzene molecular symmetry.[72,73] This symmetry reduction

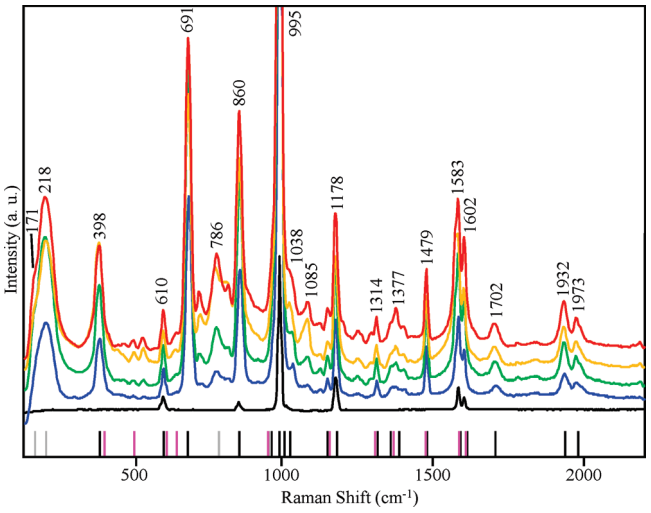

Figure 2. Raman spectra of a pristine 5 ML benzene thin film before (black) and after deposition of 5 (blue), 10 (green), 15 (orange), and 20 (red) Å mass thickness of Mg. Underlying tick marks identify characteristic frequencies for benzene (black), the benzene anion radical (pink), and the Mg−benzene adduct (gray).

occurs presumably by benzene association with the surfaces of metal nanoparticles.

Additionally, the presence of multiple new weak-intensity bands in the spectra after metal deposition suggests formation of small amounts of products from reaction between the solid-state benzene and the deposited metals. Bands at 279 and 789 cm^{-1} for Ag and at 171, 218, and 786 cm^{-1} for Mg, and a low frequency shoulder on the intense band at ~990 cm^{-1} for both metals, are suggestive of reaction chemistry between the deposited Ag or Mg and the solid-state benzene, These bands are labeled with gray tick marks beneath the spectra in Figures 1 and 2.

Theoretical and experimental studies of benzene reactions with metals of groups 1−3 and the transition metal series suggest an initial electron transfer pathway in which electrons from the metal s, p, and d orbitals are donated into the benzene π^* orbital.[74−80] The resulting benzene anion radical[78,79,81] exhibits a decrease in C−C bond order, causing ring-based vibrations such as ν_1 and ν_{19} to require less energy, resulting in a 30−50 cm^{-1} shift to lower frequencies.[22,43,45,82] On this basis, the low frequency shoulder on the ν_1 benzene bands for both Ag and Mg in Figures 1 and 2, respectively, are assigned to this shifted ν_1 mode (labeled as $\delta\nu_1$ in Table 1). A comparable band for a shifted ν_{19} mode ($\delta\nu_{19}$ in Table 1) is not observed in these spectra, consistent with the previous observation of Lyon and co-workers that the intensity of the $\delta\nu_{19}$ mode for metal−benzene anion complexes is much weaker than that of the $\delta\nu_{11}$ mode at ~790 cm^{-1} (see below for discussion of this mode.)[75]

Additional new bands in the spectra clearly indicate further reaction of this benzene anion radical with the metals to form metal−benzene adducts. Parente and co-workers[76] identified the presence of ν(M−C) bands in the region below 500 cm^{-1} as an indication of adduct formation initiated by an electron transfer reaction in their vibrational spectroscopy studies of Al-(polyacetylene) complexes. The bands at 279 cm^{-1} in the Ag/benzene spectra (Figure 1) and at 171 and 218 cm^{-1} in the Mg/benzene spectra (Figure 2) are assigned to ν(Ag−C)[82] and ν-(Mg−C)[83] modes, further substantiating the claim of metal−benzene adduct formation initiated by an electron transfer reaction.

Table 1. Raman Peak Frequencies (cm^{-1}) and Assignments for a Pristine 5 ML Benzene Thin Film before and after Deposition of Ag and Mg

observed frequency		benzene assignments[a]		metal−benzene adduct assignments[b]
		Wilson	vibrational	vibrational
Ag	Mg	notation	mode	mode
279	171			ν(M−C)
	218			
396	398	ν_{16}	$\delta(C-C-C)_{oop}$	
606	610	ν_6	$\delta(C-C-C)_{ip}$	
689	691	ν_{11}	$\delta(C-H)_{oop}$	
789	786			$\delta\nu_{11}(C-H)_{oop}$
855	860	ν_{10}	$\delta(C-H)_{oop}$	
969	967	ν_{17}	$\delta(C-H)_{oop}$	$\delta\nu_1$ $\nu(C-H)_{ring}$
987	995	ν_1	$\nu(C-H)_{ring}$	
1032	1038	ν_{18}	$\nu(C-H)_{ip}$	
1146	1151	ν_{15}	$\nu(C-H)_{ip}$	
1173	1178	ν_9	$\nu(C-H)_{ip}$	
1311	1314	ν_{14}	$\nu(C-C)_{ip}$	
1350	1350	ν_3	$\nu(C-H)_{ip}$	
1364	1377	2 x ν_{11}	2 × $\delta(C-H)_{oop}$	
1474	1479	ν_{19}	$\nu(C-C)_{ip}$	
1581	1583	ν_8	$\nu(C-C)_{ip}$	
1600	1602			
1699	1702	2 × ν_{10}	2 × $\delta(C-H)_{oop}$	
1925	1932	2 × ν_{17}	2 × $\delta(C-H)_{oop}$	
1970	1973	2 × ν_5	2 × $\delta(C-H)_{oop}$	

[a] From ref 84. [b] From refs 22, 76, and 83.

Finally, a shift of the out-of-plane ν_{11} mode from 670 cm^{-1} for benzene to 750−800 cm^{-1} has also been associated with metal−benzene adduct formation. This shift is attributed to either physical (e.g., hindrance of the out-of-plane vibrations due to a proximate metal atom)[22] or electrostatic (e.g., repulsion between $H^{\delta+}$ and $M^{\delta+}$)[82] effects of metal binding to the ring. Thus, in the spectra observed here, the band near 790 cm^{-1} for both Ag and Mg is assigned to this shifted ν_{11} mode ($\delta\nu_{11}$ in Table 1), consistent with adduct formation following an initial electron transfer reaction.

Although the presence of these new bands clearly supports metal−benzene adduct formation initiated by an electron transfer reaction, overall, these spectra are dominated by bands of unreacted benzene. It is difficult to quantify the fraction of the benzene film that undergoes reaction due to complications from surface enhancement. However, it is important to ascertain whether products continue to form as more metal is deposited or whether products form only upon initial metal deposition and then experience surface enhancement at the same rate as the unreacted benzene. In panels a and b of Figure 3, the intensity behavior of two metal−benzene adduct bands, the ν(M−C) and $\delta\nu_{11}$, are compared to two bands from unreacted benzene, the in-plane ν_9 and the out-of-plane ν_{10}, as a function of Ag and Mg mass thickness, respectively. These modes were selected because they indicate adduct formation with Ag and Mg and because each is spectrally discrete. The intensities of these bands are normalized to the most intense spectral response for that band over the

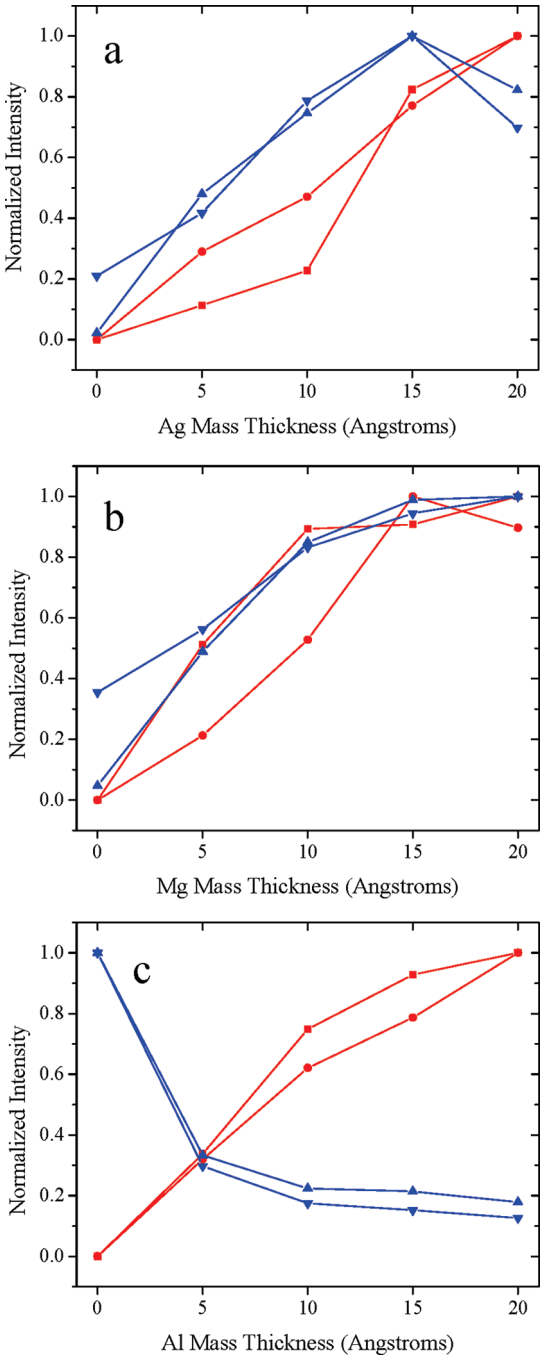

Figure 3. Intensity of unreacted benzene modes, ν_{10} (blue solid triangle up) and ν_9 (blue solid triangle down), and electron transfer product modes, ν(C−M) (red solid circle) and $\delta\nu_{11}$ (red solid square), as a function of (a) Ag,(b) Mg, and (c) Al mass thickness.

range of metal thicknesses studied. For both Ag and Mg, the normalized intensity of the metal−benzene adduct bands increases with metal mass thickness at the same rate as the unreacted benzene bands, indicating that the metal−benzene adduct is formed upon initial deposition of the metal but then ceases further formation beyond deposition of ∼5 Å of Ag or Mg.

A 5 ML film of benzene contains a total of $\sim 4.9 \times 10^{14}$ molecules/cm^2; 5 Å of Ag and Mg contain 2.0×10^{15} and 1.4×10^{15} atoms/cm^2, respectively. Thus, after deposition of only 5 Å

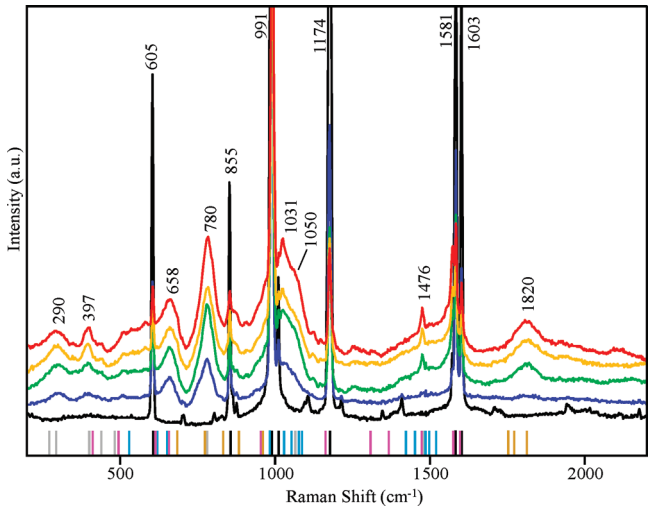

Figure 4. Raman spectra of 5 ML benzene before (black) and after deposition of 5 (blue), 10 (green), 15 (orange), and 20 (red) Å mass thickness of Al. Underlying tick marks identify characteristic frequencies for benzene (black), the benzene anion radical (pink), the Al−benzene adduct (gray), Al−H (tan), and substituted benzenes (aqua).

of metal, the metal:benzene ratio is >2:1. Since the spectra are still dominated by bands due to unreacted benzene, one can therefore conclude that only a small fraction of the total number of benzene molecules reacts with metal. Given this limited reactivity, the metal−benzene adduct is only formed in small amounts. As additional metal is deposited, metal nanoparticles must form that provide surface enhancement of both unreacted benzene and the metal−benzene adduct.

Reaction of Al with Benzene. Figure 4 shows spectra from a pristene benzene film before and after deposition of 5, 10, 15, and 20 Å mass thickness of Al. Although bands due to unreacted benzene remain in the spectra after Al deposition (identified as black tick marks under the spectra), multiple, prominent new bands are observed at 290, 397, 658, 780, 1030, 1476, and 1820 cm^{-1}. Table 2 reports the observed peak frequencies as well as characteristic frequencies for benzene,[84] the benzene anion radical[85] electron transfer products,[22,76] substituted benzenes,[86] and ν(Al−H) modes.[87−89] As discussed above, the appearance of bands at 290 and 780 cm^{-1} clearly substantiate the formation of an Al−benzene adduct initiated by an electron transfer reaction, similar to the reactions observed with Ag and Mg. However, in contrast to the behavior with these other metals, the plot in Figure 3c shows that these Al−benzene adduct bands grow in at the expense of the unreacted benzene bands. Assuming no change in scattering cross section leads to the conclusion that about 80% of the initial benzene reacts, and given that each 5 Å deposition of Al contains 2.0×10^{15} atoms/cm^2, (Al)$_n$−benzene adducts with a stoichiometry greater than 1:1 may be present.

Extensive theoretical[25,57,90,91] and experimental[18,48,91] work has been performed on the reaction of Al atoms with benzene molecules. The calculations of McKee[25] on a 1:1 Al−benzene adduct suggest the formation of a stable 1,4-substituted Al−benzene species. Silva and Head[57] performed calculations on several structures for the 1:1 adduct and found the Al-centered boat structure, similar to the complex reported by McKee,[25] and an Al σ-bridging structure in which the Al is η^4-bound to benzene, to be isoelectronically stable.

Table 2. Raman Peak Frequencies (cm^{-1}) and Assignments for a Pristine 5 ML Benzene Thin Film before and after Deposition of Al

	benzene assignments[a]		benzene anion radical assignments[b]		adduct assignments[c]	
observed frequency	Wilson number (frequency)	vibrational mode	Wilson number (frequency)	vibrational mode	frequency	vibrational mode[d]
290					235	ν(Al−C_2H_2)
					290	ν(Al_2−C_6H_6)
397			ν_{16} (408)	δ(C−C−C)$_{oop}$	400	ν_{as}(Al−C)
450−700	ν_6 (605)	δ(C−C−C)$_{ip}$	ν_6 (496)	δ(C−C−C)$_{ip}$	445	ν(Al−C)
					486	ν(Al−C)
			ν_{11} (616)	δ(C−H)$_{oop}$	415−560	M
					605−630	Mo
			ν_4 (648)	δ(C−C−C)$_{oop}$	630−650	P
					688	δ(Al−H)
780					780	$\delta\nu_{11}$ δ(C−H)$_{oop}$
						δ(Al−H)
830					830	δ(Al−H)
855	ν_{10}	δ(C−H)$_{oop}$				
882					882	δ(Al−H)
950−1150	ν_1 (991)	ν(C−H)$_{ring}$	ν_1 (957)	ν(C−H)$_{ring}$	950	δ(Al−H)
					990−1010	Mo, Me, T
					1003−1023	P
	ν_{12} (1011)	δ(C−C−C)$_{ip}$	ν_9 (1150)	δ(C−H)$_{ip}$	1016−1040	Mo
					1020−1055	O
					1050	$\delta\nu_{18}$ ν(C−H)$_{ip}$
					1065−1082	P
1174	ν_9	ν(C−H)$_{ip}$				
1400−1600	ν_8 (1581, 1603)	ν(C−C)$_{ip}$	ν_{19} (1475)	ν(C−C)	1400−1420	P
					1430−1465	Mo, O, Me
					1476	$\delta\nu_{19}$ ν(C−H)$_{ip}$
			ν_8 (1586)	ν(C−C)	1480−1525	Mo, D, T
					1470−1510	Mo, D, T
					1480−1525	Mo, D, T
1820					1720	ν(Al−H)
					1754	ν(Al−H)
					1830	ν(Al−H)

[a] From ref 84. [b] From ref 85. [c] From refs 22, 76, 86−89. [d] Benzene substitution notations: P = para, Mo = mono, Me = meta, T = trisubstituted, O = ortho, D = disubstituted.

Related experimental studies of this reaction chemistry have also been reported. Kasai and McLeod[48] reported that a 1:1 Al−benzene adduct was isolated in a neon matrix at 4 K and detected using electron spin resonance (ESR) spectroscopy. In this complex, Al was proposed to bind to benzene in an η^2 fashion through ortho-carbon atoms. Howard and co-workers[18] later performed ESR on the 1:1 Al−benzene complex isolated in inert hydrocarbon matrixes at 77 K and proposed that the 1,4-para-disubstituted Al−benzene complex was the most stable.

Although these former studies are on the 1:1 adduct, the Brédas group has provided computational analysis on multiple systems in which Al atoms are π-conjugated with organics, including polythiophene,[92] polyene,[29] poly(*p*-phenylenevinylene),[29] and polyacetylene.[76] In these complexes, Al atoms are bound to either single or multiple carbon atoms. In addition to predicted molecular geometries and bond lengths, vibrational spectra were also predicted for many of the products.[76,93,94]

Collectively, this previous work provides a framework for understanding the reaction chemistry observed here. In Figure 4, broad bands at 290 and 397 cm^{-1} are assigned as ν(Al−C) modes, similar to bands predicted at 235, 290, 400, 445, and 450 cm^{-1} by Brédas and co-workers for disubstituted π-conjugated Al−polyacetylene[76] complexes. Characteristic frequencies for such molecules[76] are indicated by gray tick marks below the spectra in Figure 4. Moreover, single or multiple Al additions to benzene would result in bands characteristic of mono-, di-, and trisubstituted benzene. Characteristic frequencies for such species include multiple bands near 660, 1030, and 1500 cm^{-1},[86] and are identified with aqua tick marks below the spectra in Figure 4.[86]

In addition, the bands at 780, 1050, and 1476 cm^{-1} in Figure 4, similar to the metal−benzene adduct modes observed with Ag and Mg, are consistent with an Al−benzene or $(Al)_n$−benzene adducts formed through an electron transfer reaction pathway as described above.[22] van Heijnsbergen et al.[22] calculated and

obtained the infrared resonance-enhanced multiphoton photodissociation spectrum of a 1:1 gas-phase Al^+—benzene adduct. In these calculations, the ν_{11}, ν_{18}, and ν_{19} modes were predicted to appear at 760, 1054, and 1509 cm^{-1}, close in value to the frequencies of 730 and 1481 cm^{-1} at which the ν_{11} and ν_{19} modes were observed, respectively, although the ν_{18} mode was too weak to be detected.[22] The rationale for these shifts was discussed above. Thus, in Figure 4, the bands at 780, 1050, and 1476 cm^{-1} are assigned to the $\delta\nu_{11}$, $\delta\nu_{18}$, and $\delta\nu_{19}$ modes of Al-substituted benzene, respectively, and the characteristic frequencies for these adducts[22] are indicated by gray tick marks below the spectra in Figure 4. In summary, the spectra in Figure 4 support formation of $(Al)_n$—benzene adducts through a pathway in which an electron is transferred from Al into the π^* orbitals of benzene resulting in single or multiple (i.e., mono-, di-, and tri-) benzene substitution in the adducts formed.[22,76,86]

Finally, a band at the unusual frequency of 1820 cm^{-1} is also observed in the spectra after postdeposition of Al. This band is assigned to an ν(Al—H) mode based on the observation of similar bands at 1830 cm^{-1} for $LiAlH_4$[89] and at 1800 cm^{-1} for dialkylaluminum hydrides.[88] As indicated in Table 2, several other modes at 688, 780, 830, 882, and 950 cm^{-1} are also characteristic of these species and are labeled as tan tick marks below the spectra.[87] Although the 1820 cm^{-1} band is observed without spectral interference, the other modes expected from the presence of Al—H moieties are superimposed on the broad bands between 450 and 700 and 950—1150 cm^{-1} and are therefore difficult to uniquely distinguish.

The observation of the ν(Al—H) mode at 1820 cm^{-1} is significant in that it supports Al insertion into a benzene C—H bond. Two types of reactions of aryl-containing molecules with metals can result in metal atom insertion into an aryl—H bond.[95−97] As detailed more fully in Figure S2 of the Supporting Information, oxidative-addition involving metal-assisted C—H bond cleavage followed by formation of an η^2 metal—arene complex leads to metal atom insertion.[95,96] Alternately, electrophilic metalation, which involves electrophilic attack at the ipso-carbon to form a metal—arenium complex followed by proton elimination, can also occur, although this pathway does not result in formation of an Al—H bond.[97] Both pathways have in common the primary step in which the metal atom injects an electron into the benzene ring. This possibility is, in fact, supported by observation of the benzene anion radical in previous ESR studies of low work function metals reacting with gas-phase benzene.[79] It is difficult to decipher whether the benzene anion radical is formed in the solid-state benzene thin films studied here, as the vibrational spectrum is similar to that for neat benzene.[85] Nonetheless, characteristic frequencies for the benzene anion radical[85] are labeled by pink tick marks to illustrate the possible presence of this species in Figure 4. In general, vibrational modes of the anion radical are shifted to lower frequencies than the corresponding neutral modes, as the addition of an electron to the antibonding π^* orbital results in a more weakly bonded ring structure.[85,98,99] Although either of these pathways could result in the formation of mono-, di-, or trisubstituted $(Al)_n$-benzene adducts, only the oxidative-addition pathway would result in formation of an Al—H moiety.

Reaction Pathway. The results above indicate limited reactivity of Ag and Mg with benzene to form Ag—benzene and Mg—benzene adducts, but much more extensive, consumptive reaction of Al to form Al—benzene adducts. Although the electron affinity of an isolated benzene molecule is −1.15 eV,[100] suggesting unfavorable electron addition, Mitsui et al.[101] reported that clusters of benzene molecules, an environment similar to that found in these solid state films, have electron affinities approaching +0.84 eV, due in part to the stabilizing effects of proximate molecules. Furthermore, Oliveres-Amaya and co-workers report that the presence of a metal stabilizes the excess charge of the benzene anion, resulting in a species lower in energy than that of the neutral molecule.[102] The ionization potential (IP) for Ag and Mg is ∼7.6 eV, while that for Al is ∼6 eV.[103] The smaller IP for Al makes its donation of an electron more facile, thereby explaining its greater reactivity.

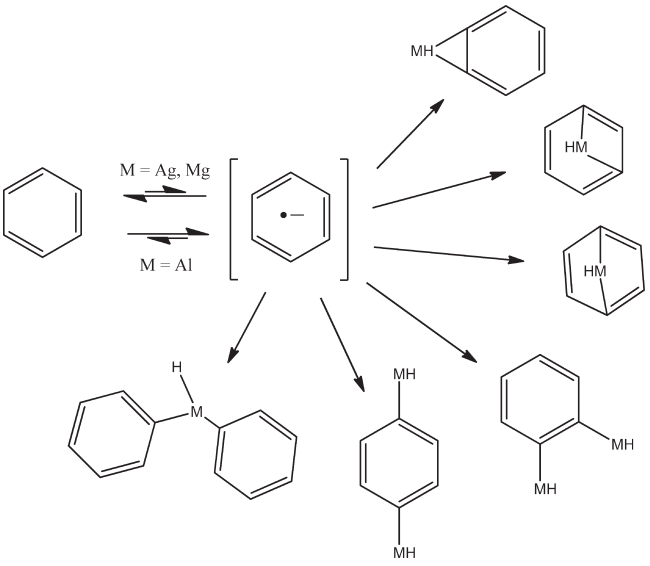

Figure 5. Proposed reaction pathway for benzene with Ag, Mg, and Al.

The proposed reaction pathway for benzene with these metals is shown in Figure 5. For Ag and Mg, the initial electron transfer reaction equilibrium lies to the left due to the relatively high IPs of these metals. Although small amounts of product with spectral signatures consistent with metal—benzene adducts (e.g., ν(M—C) and $\delta\nu_{11}$ bands) are observed with these metals, the spectra are dominated by unreacted normal benzene modes that experience surface enhancement, presumably from Ag and Mg nanoparticles. Thus, electron transfer from these metals to the average benzene molecule in these films is relatively unfavorable, leading to small amounts of metal—benzene adducts formed.

For Al, however, the electron transfer equilibrium lies to the right due to the lower ionization potential of Al, thereby creating Al^+ and a benzene anion radical. The adduct formed between these species is quite stable, with a binding constant of 35 kcal/mol.[20,23,57,59] Thus, on the basis of the spectra reported here, Al reacts with solid-state benzene at 30 K to form Al—benzene adducts as both predicted theoretically[25,57,90,91] and observed experimentally.[18,48,91] Moreover, evidence for the possible formation of $(Al)_n$—benzene adducts is not surprising, since these species are essentially isoelectronic as predicted previously by both Silva[57] and Imura.[91] Several possible product structures for the Al—benzene adducts are also shown in Figure 5.

■ ASSOCIATED CONTENT

Supporting Information. The Raman spectrum of a five monolayer, pristine, solid-state benzene film on polycrystalline Ag at 30 K along with complete vibrational assignments and

possible oxidative-addition and electrophilic metalation reaction pathways. This material is available free of charge via the Internet at http://pubs.acs.org.

AUTHOR INFORMATION

Corresponding Author

*E-mail: pembertn@u.arizona.edu.

Present Addresses

[†]Department of Chemistry, North Carolina State University, Raleigh, NC 27695.

ACKNOWLEDGMENT

Studies of the reaction of benzene with Al and Mg and preparation of this manuscript were supported as part of the Center for Interface Science: Solar Electric Materials, an Energy Frontier Research Center funded by the U.S. Department of Energy, Office of Science, Office of Basic Energy Sciences under award number DE-SC0001084. Studies of the reactions of benzene with Ag and initial studies with Al were supported by the National Science Foundation (CHE-0848624). The instrumentation for this work was supported by the National Science Foundation through grant awards (CHE-0317114 and CHE-0848624.)

REFERENCES

(1) Satoh, T. *Chem. Soc. Rev.* **2007**, *36* (10), 1561–1572.
(2) Zheng, W.; Roesky, H. W. *J. Chem. Soc., Dalton Trans.* **2002**, *14*, 2787–2796.
(3) Halbes-Letinois, U.; Weibel, J.-M.; Pale, P. *Chem. Soc. Rev.* **2007**, *36* (5), 759–769.
(4) Holloway, C. E.; Melnik, M. *J. Organomet. Chem.* **1997**, *543* (1−2), 1–37.
(5) Nagendran, S.; Roesky, H. W. *Organometallics* **2008**, *27* (4), 457–492.
(6) Crespo, O.; Gimeno, M. C.; Laguna, A. *J. Organomet. Chem.* **2009**, *694* (11), 1588–1598.
(7) Duncan, M. A. *Int. J. Mass Spectrom.* **2008**, *272* (2−3), 99–118.
(8) Flory, M. A.; Apponi, A. J.; Zack, L. N.; Ziurys, L. M. *J. Am. Chem. Soc.* **2010**, *132* (48), 17186–17192.
(9) Stockigt, D. *J. Phys. Chem. A* **1998**, *102* (51), 10493–10500.
(10) O'Hair, R. A. J.; Khairallah, G. N. *J. Cluster Sci.* **2004**, *15* (3), 331–363.
(11) Rodgers, M. T.; Armentrout, P. B. *Acc. Chem. Res.* **2004**, *37* (12), 989–998.
(12) Anderson, M. A.; Ziurys, L. M. *Astrophys. J.* **1995**, *439* (1), L25–L28.
(13) Robinson, J. S.; Ziurys, L. M. *Astrophys. J.* **1996**, *472* (2), L131–L134.
(14) Ziurys, L. M. *Proc. Natl. Acad. Sci. U.S.A.* **2006**, *103* (33), 12274–12279.
(15) Power, I. M.; Wilson, S. A.; Thom, J. M.; Dipple, G. M.; Gabites, J. E.; Southam, G. *Chem. Geol.* **2009**, *260* (3−4), 286–300.
(16) Roy, R. L.; Campbell, P. G. C.; Prémont, S.; Labrie, J. *Environ. Toxicol. Chem.* **2000**, *19* (10), 2457–2466.
(17) Himmel, H.-J. *Chem.—Eur. J.* **2004**, *10* (11), 2851–2857.
(18) Howard, J. A.; Joly, H. A.; Mile, B. *J. Am. Chem. Soc.* **1989**, *111* (21), 8094–8098.
(19) Kasai, P. H. *J. Phys. Chem. A* **1998**, *120* (31), 7884–7892.
(20) Bouchard, F.; Brenner, V.; Carra, C.; Hepburn, J. W.; Koyanagi, G. K.; McMahon, T. B.; Ohanessian, G.; Peschke, M. *J. Phys. Chem. A* **1997**, *101* (33), 5885–5894.
(21) Caraiman, D.; Koyanagi, G. K.; Bohme, D. K. *J. Phys. Chem. A* **2004**, *108* (6), 978–986.
(22) van Heijnsbergen, D.; Jaeger, T. D.; von Helden, G.; Meijer, G.; Duncan, M. A. *Chem. Phys. Lett.* **2002**, *364* (3−4), 345–351.
(23) Dunbar, R. C.; Klippenstein, S. J.; Hrusak, J.; Stockigt, D.; Schwarz, H. *J. Am. Chem. Soc.* **1996**, *118* (22), 5277–5283.
(24) Fangstrom, T.; Eriksson, L. A.; Lunell, S. *J. Phys. Chem. A* **1997**, *101* (26), 4814–4820.
(25) McKee, M. L. *J. Phys. Chem.* **1991**, *95* (19), 7247–7253.
(26) McKee, M. L. *J. Am. Chem. Soc.* **1993**, *115* (21), 9608–9613.
(27) Miyajima, K.; Yabushita, S.; Knickelbein, M. B.; Nakajima, A. *J. Am. Chem. Soc.* **2007**, *129* (27), 8473–8480.
(28) Calderone, A.; Lazzaroni, R.; Brédas, J.-L. *Macromol. Theory Simul.* **1998**, *7* (5), 509–520.
(29) Fredriksson, C.; Bredas, J. L. *J. Chem. Phys.* **1993**, *98* (5), 4253–4262.
(30) Hawkridge, A. M.; Pemberton, J. E. *J. Am. Chem. Soc.* **2002**, *125* (3), 624–625.
(31) Davis, R. J.; Pemberton, J. E. *J. Phys. Chem. C* **2008**, *112* (11), 4364–4371.
(32) Davis, R. J.; Pemberton, J. E. *J. Am. Chem. Soc.* **2009**, *131* (29), 10009–10014.
(33) Davis, R. J.; Pemberton, J. E. *J. Phys. Chem. A* **2009**, *113* (16), 4397–4402.
(34) Alberti, M.; Aguilar, A.; Lucas, J. M.; Lagana, A.; Pirani, F. *J. Phys. Chem. A* **2007**, *111* (10), 1780–1787.
(35) Cheng, J.; Zhu, W.; Tang, Y.; Xu, Y.; Li, Z.; Chen, K.; Jiang, H. *Chem. Phys. Lett.* **2006**, *422* (4−6), 455–460.
(36) Hanusa, T. P. *Polyhedron* **1990**, *9* (11), 1345–1362.
(37) Kress, J.; Novak, A. *J. Organomet. Chem.* **1976**, *121* (1), 7–18.
(38) Miljanic, S.; Frkanec, L.; Biljan, T.; Meic, Z.; Zinic, M. *Langmuir* **2006**, *22*, 9079–9081.
(39) Pessôa, M. M. B.; Temperini, M. L. A. *J. Raman Spectrosc.* **2002**, *33* (1), 50–55.
(40) Taufen, H. J.; Murray, M. J.; Cleveland, F. F. *J. Am. Chem. Soc.* **1941**, *63* (12), 3500–3503.
(41) Chen, Y.-M.; Armentrout, P. B. *Chem. Phys. Lett.* **1993**, *210* (1−3), 123–128.
(42) Duncan, M. A. *Int. Rev. Phys. Chem.* **2003**, *22* (2), 407–435.
(43) Jaeger, T. D.; van Heijnsbergen, D.; Klippenstein, S. J.; von Helden, G.; Meijer, G.; Duncan, M. A. *J. Am. Chem. Soc.* **2004**, *126* (35), 10981–10991.
(44) Koretsky, G. M.; Knickelbein, M. B. *Chem. Phys. Lett.* **1997**, *267* (5−6), 485–490.
(45) van Heijnsbergen, D.; von Helden, G.; Meijer, G.; Maitre, P.; Duncan, M. A. *J. Am. Chem. Soc.* **2002**, *124* (8), 1562–1563.
(46) Willey, K. F.; Cheng, P. Y.; Pearce, K. D.; Duncan, M. A. *J. Phys. Chem.* **1990**, *94* (12), 4769–4772.
(47) Kasai, P. H. *J. Am. Chem. Soc.* **1982**, *104* (5), 1165–1172.
(48) Kasai, P. H.; McLeod, D. *J. Am. Chem. Soc.* **1979**, *101* (19), 5860–5862.
(49) Bauschlicher, C. W.; Partridge, H.; Langhoff, S. R. *J. Phys. Chem.* **1992**, *96* (8), 3273–3278.
(50) Chen, R.; Cheng, Y.-H.; Li, X.-S.; Guo, Q.-X. *Res. Chem. Intermed.* **2002**, *28* (1), 41.
(51) Dargel, T. K.; Hertwig, R. H.; Koch, W. *Mol. Phys.* **1999**, *96* (4), 583–591.
(52) Fu, A. P.; Du, D. M.; Zhou, Z. Y. *Chin. Chem. Lett.* **2000**, *11* (3), 219–222.
(53) Mishra, B. K.; Bajpai, V. K.; Ramanathan, V.; Gadre, S. R.; Sathyamurthy, N. *Mol. Phys.* **2008**, *106* (12−13), 1557–1566.
(54) Mitchell, S. A.; Simard, B.; Rayner, D. M.; Hackett, P. A. *J. Phys. Chem.* **1988**, *92* (6), 1655–1664.
(55) Petrie, S. *Int. J. Mass Spectrom.* **2003**, *227* (1), 33–46.
(56) Reddy, A. S.; Vijay, D.; Sastry, G. M.; Sastry, G. N. *J. Phys. Chem. B* **2006**, *110* (6), 2479–2481.
(57) Silva, S. J.; Head, J. D. *J. Am. Chem. Soc.* **1992**, *114* (16), 6479–6484.
(58) Soteras, I.; Orozco, M.; Luque, F. J. *Phys. Chem. Chem. Phys.* **2008**, *10* (19), 2616–2624.

(59) Stockigt, D. *J. Phys. Chem. A* **1997**, *101* (20), 3800–3807.
(60) Tan, X. J.; Zhu, W. L.; Cui, M.; Luo, X. M.; Gu, J. D.; Silman, I.; Sussman, J. L.; Jiang, H. L.; Ji, R. Y.; Chen, K. X. *Chem. Phys. Lett.* **2001**, *349* (1−2), 113–122.
(61) Vijay, D.; Sastry, G. N. *Phys. Chem. Chem. Phys.* **2008**, *10* (4), 582–590.
(62) Zeng, K.; Zhang, J.-L.; Cao, Z.-X.; Zhang, Q.-E. *Chin. J. Struct. Chem.* **2004**, *23* (9), 1051–1055.
(63) Zhao, Y. L.; Lin, C. S.; Zhang, R. Q.; Wang, R. S. *J. Chem. Phys.* **2005**, *122* (19), 194322.
(64) Smolinski, S.; Zelenay, P.; Sobkowski, J. *J. Electroanal. Chem.* **1998**, *442* (1−2), 41–47.
(65) Tiani, D. J.; Pemberton, J. E. *Langmuir* **2003**, *19* (16), 6422–6429.
(66) Mills, I.; Cvitas, T.; Homann, K.; Kallay, N.; Kuchitsu, K. *Quantities, Units, and Symbols in Physical Chemistry*, 2nd ed.; Blackwell Science, Ltd.: Oxford, 1993.
(67) Ishii, K.; Nakayama, H.; Yoshida, T.; Usui, H.; Koyama, K. *Bull. Chem. Soc. Jpn.* **1996**, *69* (10), 2831–2838.
(68) Moskovits, M.; Dilella, D. P. *J. Chem. Phys.* **1980**, *73* (12), 6068–6075.
(69) Wolkow, R. A.; Moskovits, M. *J. Chem. Phys.* **1992**, *96* (5), 3966–3980.
(70) Avouris, P.; Demuth, J. E. *J. Chem. Phys.* **1981**, *75* (10), 4783–4794.
(71) Koel, B. E.; Crowell, J. E.; Mate, C. M.; Somorjai, G. A. *J. Phys. Chem.* **1984**, *88* (10), 1988–1996.
(72) Grabhorn, H.; Otto, A. *Vacuum* **1990**, *41* (1−3), 473–475.
(73) Hallmark, V. M.; Campion, A. *Chem. Phys. Lett.* **1984**, *110* (6), 561–564.
(74) Dannetun, P.; Logdlund, M.; Fredriksson, C.; Lazzaroni, R.; Fauquet, C.; Stafstrom, S.; Spangler, C. W.; Bredas, J. L.; Salaneck, W. R. *J. Chem. Phys.* **1994**, *100* (9), 6765–6771.
(75) Lyon, J. T.; Andrews, L. *J. Phys. Chem. A* **2004**, *109* (3), 431–440.
(76) Parente, V.; Fredriksson, C.; Selmani, A.; Lazzaroni, R.; Bredas, J. L. *J. Phys. Chem. B* **1997**, *101* (21), 4193–4202.
(77) Chaquin, P.; Costa, D.; Lepetit, C.; Che, M. *J. Phys. Chem. A* **2001**, *105* (18), 4541–4545.
(78) Mochida, K.; Mizuno, Y. *Chem. Lett.* **1986**, *15* (7), 1125–1128.
(79) Mochida, K.; Mizuno, Y. *Bull. Chem. Soc. Jpn.* **1987**, *60* (1), 273–276.
(80) Katsenis, A. D.; Kessler, V. G.; Papaefstathiou, G. S. *Dalton Trans.* **2011**, *40* (17), 4590–4598.
(81) Mochida, K.; Takeuchi, K.; Hiraga, Y.; Ogawa, H. *Organometallics* **1987**, *6* (11), 2293–2297.
(82) Stanghellini, P. L.; Diana, E.; Arrais, A.; Rossin, A.; Kettle, S. F. A. *Organometallics* **2006**, *25* (21), 5024–5030.
(83) Lippincott, E. R.; Xavier, J.; Steele, D. *J. Am. Chem. Soc.* **1961**, *83* (10), 2262–2266.
(84) Varsanyi, G. *Vibrational Spectra of Benzene Derivatives*; Academic Press: New York, 1969.
(85) Moore, J. C.; Thornton, C.; Collier, W. B.; Devlin, J. P. *J. Phys. Chem.* **1981**, *85* (4), 350–354.
(86) Lin-Vien, D.; Colthup, N. B.; Fateley, W. G.; Grasselli, J. G. *The Handbook of Infrared and Raman Characteristic Frequencies of Organic Molecules*; Acedemic Press, Inc.: Boston, 1991.
(87) Chellappa, R. S.; Chandra, D.; Gramsch, S. A.; Hemley, R. J.; Lin, J.-F.; Song, Y. *J. Phys. Chem. B* **2006**, *110* (23), 11088–11097.
(88) Hoffman, E. G.; Schomberg, G. *Z. Elektrochem.* **1957**, *61*, 1101.
(89) Seballos, L.; Newhouse, R.; Zhang, J. Z.; Majzoub, E.; Ronnebro, E. *Proc. SPIE* **2007**, *6650*, 66500N.
(90) Fredriksson, C.; Stafstrom, S.; Dannetun, P.; Fauquet, C.; Salaneck, W. R.; Lazzaroni, R.; Bredas, J.-L.; Ouhlal, A.; Selmani, A. *Plast. Eng.* **1998**, *43*, 199–211.
(91) Imura, K.; Kawashima, T.; Ohoyama, H.; Kasai, T.; Nakajima, A.; Kaya, K. *Phys. Chem. Chem. Phys.* **2001**, *3*, 3593–3597.
(92) Boman, M.; Stafstrom, S.; Bredas, J. L. *J. Chem. Phys.* **1992**, *97* (12), 9144–9153.
(93) Lazzaroni, R.; Parenté, V.; Fredriksson, C.; Brédas, J. L. *Synth. Met.* **1996**, *76* (1−3), 225–228.
(94) Parente, V.; Pourtois, G.; Lazzaroni, R.; Brédas, J.-L.; Ruani, G.; Murgia, M.; Zamboni, R. *Adv. Mater.* **1998**, *10* (4), 319–324.
(95) Jones, W. D.; Feher, F. J. *J. Am. Chem. Soc.* **1982**, *104* (15), 4240–4242.
(96) Jones, W. D.; Feher, F. J. *Acc. Chem. Res.* **1989**, *22* (3), 91–100.
(97) Ryabov, A. D. *Chem. Rev.* **1990**, *90* (2), 403–424.
(98) Perebeinos, V.; Allen, P. B.; Pederson, M. *Phys. Rev. A* **2005**, *72* (1), 012501.
(99) Tokunaga, K.; Sato, T.; Tanaka, K. *J. Chem. Phys.* **2006**, *124* (15), 154303.
(100) Hajgato, B.; Deleuze, M. S.; Tozer, D. J.; De Proft, F. *J. Chem. Phys.* **2008**, *129* (8), 084308.
(101) Mitsui, M.; Nakajima, A.; Kaya, K.; Even, U. *J. Chem. Phys.* **2001**, *115* (13), 5707–5710.
(102) Olivares-Amaya, R.; Stopa, M.; Andrade, X.; Watson, M. A.; Aspuru-Guzik, A. n. *J. Phys. Chem. Lett.* **2011**, *2* (7), 682–688.
(103) Lide, D. R. *Handbook of Chemistry and Physics*, 87th ed.; CRC Press: Boca Raton, FL, 2006.